

Cascade R-CNN: Delving into High Quality Object Detection

Zhaowei Cai
UC San Diego
zwcai@ucsd.edu

Nuno Vasconcelos
UC San Diego
nuno@ucsd.edu

Abstract

In object detection, an intersection over union (IoU) threshold is required to define positives and negatives. An object detector, trained with low IoU threshold, e.g. 0.5, usually produces noisy detections. However, detection performance tends to degrade with increasing the IoU thresholds. Two main factors are responsible for this: 1) overfitting during training, due to exponentially vanishing positive samples, and 2) inference-time mismatch between the IoUs for which the detector is optimal and those of the input hypotheses. A multi-stage object detection architecture, the Cascade R-CNN, is proposed to address these problems. It consists of a sequence of detectors trained with increasing IoU thresholds, to be sequentially more selective against close false positives. The detectors are trained stage by stage, leveraging the observation that the output of a detector is a good distribution for training the next higher quality detector. The resampling of progressively improved hypotheses guarantees that all detectors have a positive set of examples of equivalent size, reducing the overfitting problem. The same cascade procedure is applied at inference, enabling a closer match between the hypotheses and the detector quality of each stage. A simple implementation of the Cascade R-CNN is shown to surpass all single-model object detectors on the challenging COCO dataset. Experiments also show that the Cascade R-CNN is widely applicable across detector architectures, achieving consistent gains independently of the baseline detector strength. The code is available at <https://github.com/zhaoweicai/cascade-rcnn>.

1. Introduction

Object detection is a complex problem, requiring the solution of two main tasks. First, the detector must solve the *recognition* problem, to distinguish foreground objects from background and assign them the proper object class labels. Second, the detector must solve the *localization* problem, to assign accurate bounding boxes to different objects. Both of these are particularly difficult because the detector faces many “close” false positives, corresponding to “close but

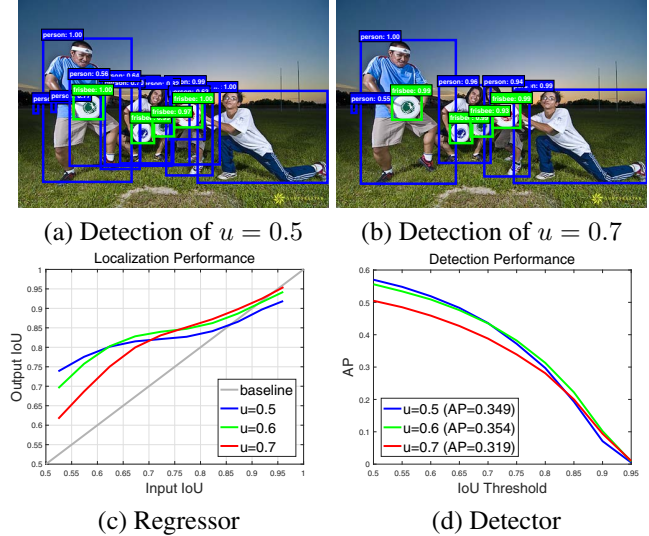


Figure 1. The detection outputs, localization and detection performance of object detectors of increasing IoU threshold u .

not correct” bounding boxes. The detector must find the true positives while suppressing these close false positives.

Many of the recently proposed object detectors are based on the two-stage R-CNN framework [14, 13, 30, 23], where detection is framed as a multi-task learning problem that combines classification and bounding box regression. Unlike object recognition, an intersection over union (IoU) threshold is required to define positives/negatives. However, the commonly used threshold values u , typically $u = 0.5$, establish quite a loose requirement for positives. The resulting detectors frequently produce noisy bounding boxes, as shown in Figure 1 (a). Hypotheses that most humans would consider close false positives frequently pass the $\text{IoU} \geq 0.5$ test. While the examples assembled under the $u = 0.5$ criterion are rich and diversified, they make it difficult to train detectors that can effectively reject close false positives.

In this work, we define the *quality* of an hypothesis as its IoU with the ground truth, and the *quality of the detector* as the IoU threshold u used to train it. The goal is to investigate the, so far, poorly researched problem of learning high quality object detectors, whose outputs contain few close

false positives, as shown in Figure 1 (b). The basic idea is that a single detector can only be optimal for a single quality level. This is known in the cost-sensitive learning literature [7, 26], where the optimization of different points of the receiver operating characteristic (ROC) requires different loss functions. The main difference is that we consider the optimization for a given IoU threshold, rather than false positive rate.

The idea is illustrated by Figure 1 (c) and (d), which present the localization and detection performance, respectively, of three detectors trained with IoU thresholds of $u = 0.5, 0.6, 0.7$. The localization performance is evaluated as a function of the IoU of the input proposals, and the detection performance as a function of IoU threshold, as in COCO [22]. Note that, in Figure 1 (c), each bounding box regressor performs best for examples of IoU close to the threshold that the detector was trained. This also holds for detection performance, up to overfitting. Figure 1 (d) shows that, the detector of $u = 0.5$ outperforms the detector of $u = 0.6$ for low IoU examples, underperforming it at higher IoU levels. In general, a detector optimized at a single IoU level is not necessarily optimal at other levels. These observations suggest that higher quality detection requires a closer quality *match* between the detector and the hypotheses that it processes. In general, a detector can only have high quality if presented with high quality proposals.

However, to produce a high quality detector, it does not suffice to simply increase u during training. In fact, as seen for the detector of $u = 0.7$ of Figure 1 (d), this can degrade detection performance. The problem is that the distribution of hypotheses out of a proposal detector is usually heavily imbalanced towards low quality. In general, forcing larger IoU thresholds leads to an exponentially smaller numbers of positive training samples. This is particularly problematic for neural networks, which are known to be very example intensive, and makes the “high u ” training strategy quite prone to overfitting. Another difficulty is the mismatch between the quality of the detector and that of the testing hypotheses at inference. As shown in Figure 1, high quality detectors are only necessarily optimal for high quality hypotheses. The detection could be suboptimal when they are asked to work on the hypotheses of other quality levels.

In this paper, we propose a new detector architecture, Cascade R-CNN, that addresses these problems. It is a multi-stage extension of the R-CNN, where detector stages deeper into the cascade are sequentially more selective against close false positives. The cascade of R-CNN stages are trained sequentially, using the output of one stage to train the next. This is motivated by the observation that the output IoU of a regressor is almost invariably better than the input IoU, in Figure 1 (c), where nearly all plots are above the gray line. It suggests that the output of a detector trained with a certain IoU threshold is a good distribution to

train the detector of the next higher IoU threshold. This is similar to *bootstrapping* methods commonly used to assemble datasets in object detection literature [34, 9]. The main difference is that the resampling procedure of the Cascade R-CNN does not aim to mine hard negatives. Instead, by adjusting bounding boxes, each stage aims to find a good set of close false positives for training the next stage. When operating in this manner, a sequence of detectors adapted to increasingly higher IoUs can beat the overfitting problem, and thus be effectively trained. At inference, the same cascade procedure is applied. The progressively improved hypotheses are better matched to the increasing detector quality at each stage. This enables higher detection accuracies, as suggested by Figure 1 (c) and (d).

The Cascade R-CNN is quite simple to implement and trained end-to-end. Our results show that a vanilla implementation, without any bells and whistles, surpasses all previous state-of-the-art *single-model* detectors by a large margin, on the challenging COCO detection task [22], especially under the higher quality evaluation metrics. In addition, the Cascade R-CNN can be built with any two-stage object detector based on the R-CNN framework. We have observed consistent gains (of 2~4 points), at a marginal increase in computation. This gain is independent of the strength of the baseline object detectors. We thus believe that this simple and effective detection architecture can be of interest for many object detection research efforts.

2. Related Work

Due to the success of the R-CNN [14] architecture, the two-stage detection framework, by combining a proposal detector and a region-wise classifier, has become predominant in the recent past. To reduce redundant CNN computations in the R-CNN for speeds-up, the SPP-Net [17] and Fast R-CNN [13] introduced the idea of region-wise feature extraction. Later, the Faster R-CNN [30] achieved further speeds-up by introducing a Region Proposal Network (RPN). Some more recent works have extended it to address various problems of detail. For example, the R-FCN [4] proposed efficient region-wise fully convolutions without accuracy loss, to avoid the heavy region-wise CNN computations of the Faster R-CNN; while the MS-CNN [1] and FPN [23] detect high-recall proposals at multiple output layers, so as to alleviate the scale mismatch between the RPN receptive fields and actual object size.

Alternatively, one-stage object detection architectures have also become popular, mostly due to their computational efficiency. YOLO [29] outputs very sparse detection results and enables real time object detection, by forwarding the input image once through an efficient backbone network. SSD [25] detects objects in a way similar to the RPN [30], but uses multiple feature maps at different resolutions to cover objects at various scales. Their main limitation is

that their accuracies are typically below that of two-stage detectors. Recently, RetinaNet [24] was proposed to address the extreme foreground-background class imbalance in dense object detection, achieving better results than state-of-the-art two-stage object detectors.

Some explorations in multi-stage object detection have also been proposed. The multi-region detector [10] introduced *iterative bounding box regression*, where a R-CNN is applied several times, to produce better bounding boxes. [36, 12, 11] used a multi-stage procedure to generate accurate proposals, and forwarded them to an accurate model (e.g. Fast R-CNN). [37, 27] also attempted to localize objects sequentially. However, these methods usually used the *same* regressor iteratively for accurate localization. [21, 28] embedded the classic cascade architecture of [34] in object detection networks. [3] iterated a detection and a segmentation task alternatively, for instance segmentation.

3. Object Detection

In this paper, we extend the two-stage architecture of the Faster R-CNN [30, 23], shown in Figure 3 (a). The first stage is a proposal sub-network (“H0”), applied to the entire image, to produce preliminary detection hypotheses, known as object proposals. In the second stage, these hypotheses are then processed by a region-of-interest detection sub-network (“H1”), denoted as detection head. A final classification score (“C”) and a bounding box (“B”) are assigned to each hypothesis. We focus on modeling a multi-stage detection sub-network, and adopt, but are not limited to, the RPN [30] for proposal detection.

3.1. Bounding Box Regression

A bounding box $\mathbf{b} = (b_x, b_y, b_w, b_h)$ contains the four coordinates of an image patch x . The task of bounding box regression is to regress a candidate bounding box \mathbf{b} into a target bounding box \mathbf{g} , using a regressor $f(x, \mathbf{b})$. This is learned from a training sample $(\mathbf{g}_i, \mathbf{b}_i)$, so as to minimize the bounding box L_1 loss function, $L_{loc}(f(x_i, \mathbf{b}_i), \mathbf{g}_i)$, as suggested in Fast R-CNN [13]. To encourage a regression invariant to scale and location, L_{loc} operates on the distance vector $\Delta = (\delta_x, \delta_y, \delta_w, \delta_h)$ defined by

$$\begin{aligned} \delta_x &= (g_x - b_x)/b_w, & \delta_y &= (g_y - b_y)/b_h \\ \delta_w &= \log(g_w/b_w), & \delta_h &= \log(g_h/b_h). \end{aligned} \quad (1)$$

Since bounding box regression usually performs minor adjustments on b , the numerical values of (1) can be very small. Hence, the regression loss is usually much smaller than the classification loss. To improve the effectiveness of multi-task learning, Δ is usually normalized by its mean and variance, i.e. δ_x is replaced by $\delta'_x = (\delta_x - \mu_x)/\sigma_x$. This is widely used in the literature [30, 1, 4, 23, 16].

Some works [10, 11, 18] have argued that a single regression step of f is insufficient for accurate localization.

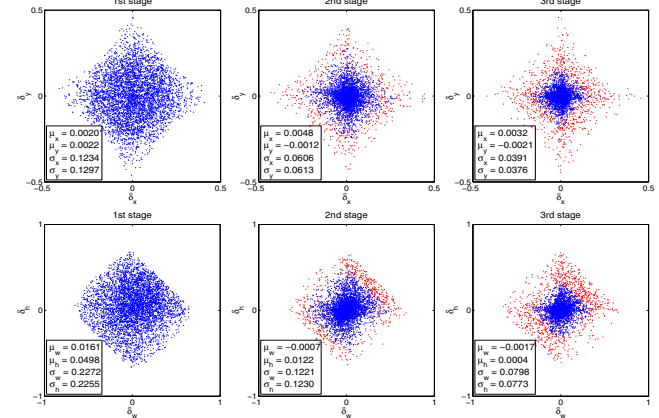


Figure 2. Sequential Δ distribution (without normalization) at different cascade stage. Red dots are outliers when using increasing IoU thresholds, and the statistics are obtained after outlier removal.

Instead, f is applied iteratively, as a post-processing step

$$f'(x, \mathbf{b}) = f \circ f \circ \dots \circ f(x, \mathbf{b}), \quad (2)$$

to refine a bounding box \mathbf{b} . This is called *iterative bounding box regression*, denoted as *iterative BBox*. It can be implemented with the inference architecture of Figure 3 (b) where all heads are the *same*. This idea, however, ignores two problems. First, as shown in Figure 1, a regressor f trained at $u = 0.5$, is suboptimal for hypotheses of higher IoUs. It actually *degrades* bounding boxes of IoU larger than 0.85. Second, as shown in Figure 2, the distribution of bounding boxes changes significantly after each iteration. While the regressor is optimal for the initial distribution it can be quite suboptimal after that. Due to these problems, *iterative BBox* requires a fair amount of human engineering, in the form of proposal accumulation, box voting, etc. [10, 11, 18], and has somewhat unreliable gains. Usually, there is no benefit beyond applying f twice.

3.2. Detection Quality

The classifier $h(x)$ assigns an image patch x to one of $M + 1$ classes, where class 0 contains background and the remaining the objects to detect. Given a training set (x_i, y_i) , it is learned by minimizing a classification cross-entropy loss $L_{cls}(h(x_i), y_i)$, where y_i is the class label of patch x_i .

Since a bounding box usually includes an object and some amount of background, it is difficult to determine if a detection is positive or negative. This is usually addressed by the IoU metric. If the IoU is above a threshold u , the patch is considered an example of the class. Thus, the class label of a hypothesis x is a function of u ,

$$y = \begin{cases} g_y, & IoU(x, g) \geq u \\ 0, & \text{otherwise} \end{cases} \quad (3)$$

where g_y is the class label of the ground truth object g . This IoU threshold u defines the quality of a detector.

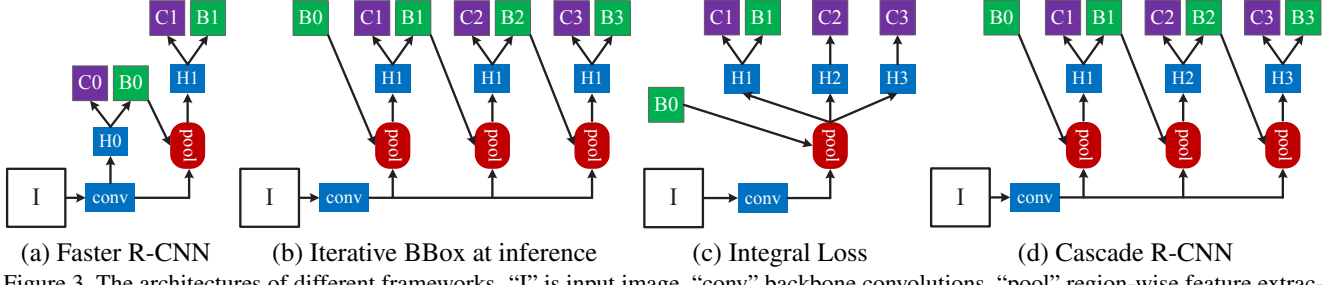


Figure 3. The architectures of different frameworks. “I” is input image, “conv” backbone convolutions, “pool” region-wise feature extraction, “H” network head, “B” bounding box, and “C” classification. “B0” is proposals in all architectures.

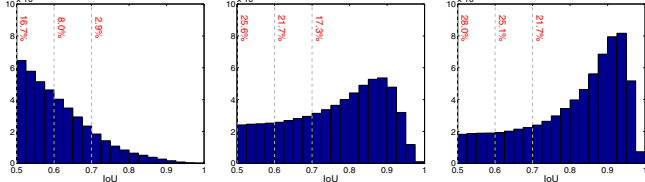


Figure 4. The IoU histogram of training samples. The distribution at 1st stage is the output of RPN. The red numbers are the positive percentage higher than the corresponding IoU threshold.

Object detection is challenging because, no matter threshold, the detection setting is highly adversarial. When u is high, the positives contain less background, but it is difficult to assemble enough positive training examples. When u is low, a richer and more diversified positive training set is available, but the trained detector has little incentive to reject close false positives. In general, it is very difficult to ask a single classifier to perform uniformly well over all IoU levels. At inference, since the majority of the hypotheses produced by a proposal detector, e.g. RPN [30] or selective search [33], have low quality, the detector must be more discriminant for lower quality hypotheses. A standard compromise between these conflicting requirements is to settle on $u = 0.5$. This, however, is a relatively low threshold, leading to low quality detections that most humans consider close false positives, as shown in Figure 1 (a).

A naïve solution is to develop an ensemble of classifiers, with the architecture of Figure 3 (c), optimized with a loss that targets various quality levels,

$$L_{cls}(h(x), y) = \sum_{u \in U} L_{cls}(h_u(x), y_u), \quad (4)$$

where U is a set of IoU thresholds. This is closely related to the *integral loss* of [38], where $U = \{0.5, 0.55, \dots, 0.75\}$, designed to fit the evaluation metric of the COCO challenge. By definition, the classifiers need to be ensembled at inference. This solution fails to address the problem that the different losses of (4) operate on different numbers of positives. As shown in the first figure of Figure 4, the set of positive samples decreases quickly with u . This is particularly problematic because the high quality classifiers are prone to overfitting. In addition, those high quality classifi-

fers are required to process proposals of overwhelming low quality at inference, for which they are not optimized. Due to all this, the ensemble of (4) fails to achieve higher accuracy at most quality levels, and the architecture has very little gain over that of Figure 3 (a).

4. Cascade R-CNN

In this section we introduce the proposed Cascade R-CNN object detection architecture of Figure 3 (d).

4.1. Cascaded Bounding Box Regression

As seen in Figure 1 (c), it is very difficult to ask a single regressor to perform perfectly uniformly at all quality levels. The difficult regression task can be decomposed into a sequence of simpler steps, inspired by the works of cascade pose regression [6] and face alignment [2, 35]. In the Cascade R-CNN, it is framed as a cascaded regression problem, with the architecture of Figure 3 (d). This relies on a cascade of *specialized* regressors

$$f(x, \mathbf{b}) = f_T \circ f_{T-1} \circ \dots \circ f_1(x, \mathbf{b}), \quad (5)$$

where T is the total number of cascade stages. Note that each regressor f_t in the cascade is optimized *w.r.t.* the sample distribution $\{\mathbf{b}^t\}$ arriving at the corresponding stage, instead of the initial distribution of $\{\mathbf{b}^1\}$. This cascade improves hypotheses progressively.

It differs from the *iterative BBox* architecture of Figure 3 (b) in several ways. First, while *iterative BBox* is a post-processing procedure used to improve bounding boxes, cascaded regression is a *resampling* procedure that changes the distribution of hypotheses to be processed by the different stages. Second, because it is used at both training and inference, there is no discrepancy between training and inference distributions. Third, the multiple specialized regressors $\{f_T, f_{T-1}, \dots, f_1\}$ are optimized for the *resampled distributions* of the different stages. This opposes to the single f of (2), which is only optimal for the initial distribution. These differences enable more precise localization than *iterative BBox*, with no further human engineering.

As discussed in Section 3.1, $\Delta = (\delta_x, \delta_y, \delta_w, \delta_h)$ in (1) needs to be normalized for effective multi-task learning. Af-

ter each regression stage, their statistics will evolve sequentially, as displayed in Figure 2. At training, the corresponding statistics are used to normalize Δ at each stage.

4.2. Cascaded Detection

As shown in the left of Figure 4, the distribution of the initial hypotheses, e.g. RPN proposals, is heavily tilted towards low quality. This inevitably induces ineffective learning of higher quality classifiers. The Cascade R-CNN addresses the problem by relying on cascade regression as a *resampling mechanism*. This is motivated by the fact that in Figure 1 (c) nearly all curves are above the diagonal gray line, i.e. a bounding box regressor trained for a certain u tends to produce bounding boxes of *higher* IoU. Hence, starting from a set of examples (x_i, \mathbf{b}_i) , cascade regression successively resamples an example distribution (x'_i, \mathbf{b}'_i) of higher IoU. In this manner, it is possible to keep the set of positive examples of the successive stages at a roughly *constant* size, even when the detector quality (IoU threshold) is *increased*. This is illustrated in Figure 4, where the distribution tilts more heavily towards high quality examples after each resampling step. Two consequences ensue. First, there is no overfitting, since positive examples are plentiful at all levels. Second, the detectors of the deeper stages are optimized for higher IoU thresholds. Note that, some outliers are sequentially removed by increasing IoU thresholds, as illustrated in Figure 2, enabling a better trained sequence of specialized detectors.

At each stage t , the R-CNN includes a classifier h_t and a regressor f_t optimized for IoU threshold u^t , where $u^t > u^{t-1}$. This is learned by minimizing the loss

$$L(x^t, g) = L_{cls}(h_t(x^t), y^t) + \lambda[y^t \geq 1]L_{loc}(f_t(x^t, \mathbf{b}^t), \mathbf{g}), \quad (6)$$

where $\mathbf{b}^t = f_{t-1}(x^{t-1}, \mathbf{b}^{t-1})$, g is the ground truth object for x^t , $\lambda = 1$ the trade-off coefficient, $[.]$ the indicator function, and y^t is the label of x^t given u^t by (3). Unlike the *integral loss* of (4), this guarantees a sequence of effectively trained detectors of increasing quality. At inference, the quality of the hypotheses is sequentially improved, by applications of the same cascade procedure, and higher quality detectors are only required to operate on higher quality hypotheses. This enables high quality object detection, as suggested by Figure 1 (c) and (d).

5. Experimental Results

The Cascade R-CNN was evaluated mainly on MS-COCO 2017 [22], which contains $\sim 118k$ images for training, $5k$ for validation (`val`) and $\sim 20k$ for testing without provided annotations (`test-dev`). The COCO-style Average Precision (AP) averages AP across IoU thresholds from 0.5 to 0.95 with an interval of 0.05 . These metrics measure the detection performance of various qualities. All models

were trained on COCO training set, and evaluated on `val` set. Final results were also reported on `test-dev` set.

5.1. Implementation Details

All regressors are class agnostic for simplicity. All cascade detection stages in Cascade R-CNN have the same architecture, which is the head of the baseline detection network. In total, Cascade R-CNN have four stages, one RPN and three for detection with $U = \{0.5, 0.6, 0.7\}$, unless otherwise noted. The sampling of the first detection stage follows [13, 30]. In the following stages, resampling is implemented by simply using the regressed outputs from the previous stage, as in Section 4.2. No data augmentation was used except standard horizontal image flipping. Inference was performed on a single image scale, with no further bells and whistles. All baseline detectors were reimplemented with Caffe [20], on the same codebase for fair comparison.

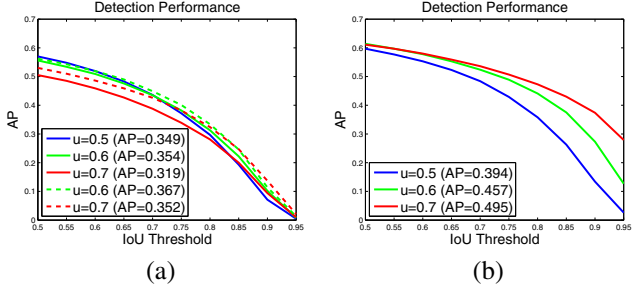
5.1.1 Baseline Networks

To test the versatility of the Cascade R-CNN, experiments were performed with three popular baseline detectors: Faster R-CNN with backbone VGG-Net [32], R-FCN [4] and FPN [23] with ResNet backbone [18]. These baselines have a wide range of detection performances. Unless noted, their default settings were used. End-to-end training was used instead of multi-step training.

Faster R-CNN: The network head has two fully connected layers. To reduce parameters, we used [15] to prune less important connections. 2048 units were retained per fully connected layer and dropout layers were removed. Training started with a learning rate of 0.002, reduced by a factor of 10 at 60k and 90k iterations, and stopped at 100k iterations, on 2 synchronized GPUs, each holding 4 images per iteration. 128 RoIs were used per image.

R-FCN: R-FCN adds a convolutional, a bounding box regression, and a classification layer to the ResNet. All heads of the Cascade R-CNN have this structure. Online hard negative mining [31] was not used. Training started with a learning rate of 0.003, which was decreased by a factor of 10 at 160k and 240k iterations, and stopped at 280k iterations, on 4 synchronized GPUs, each holding one image per iteration. 256 RoIs were used per image.

FPN: Since no source code was publicly available for FPN, our implementation details could be different. RoIAlign [16] was used for a stronger baseline. This is denoted as FPN+ and was used in all ablation studies. As usual, ResNet-50 was used for ablation studies, and ResNet-101 for final detection. Training used a learning rate of 0.005 for 120k iterations and 0.0005 for the next 60k iterations, on 8 synchronized GPUs, each holding one image per iteration. 256 RoIs were used per image.



(a)

(b)

Figure 5. (a) is detection performance of individually trained detectors, with their own proposals (solid curves) or Cascade R-CNN stage proposals (dashed curves), and (b) is by adding ground truth to the proposal set.

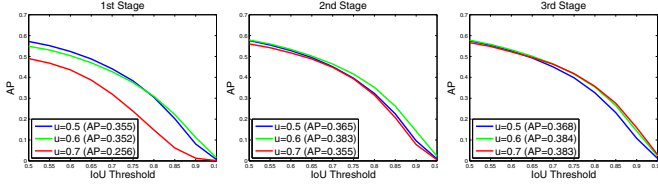
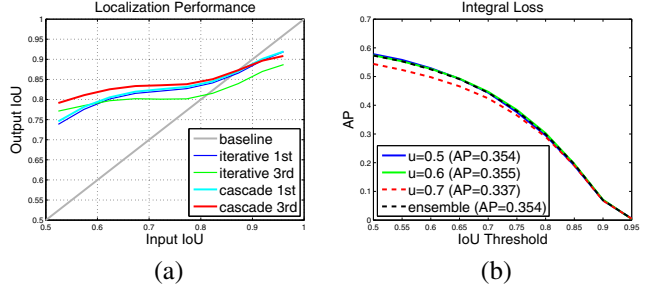


Figure 6. The detection performance of all Cascade R-CNN detectors at all cascade stages.

5.2. Quality Mismatch

Figure 5 (a) shows the AP curves of three individually trained detectors of increasing IoU thresholds of $U = \{0.5, 0.6, 0.7\}$. The detector of $u = 0.5$ outperforms the detector of $u = 0.6$ at low IoU levels, but underperforms it at higher levels. However, the detector of $u = 0.7$ underperforms the other two. To understand why this happens, we changed the quality of the proposals at inference. Figure 5 (b) shows the results obtained when ground truth bounding boxes were added to the set of proposals. While all detectors improve, the detector of $u = 0.7$ has the largest gains, achieving the best performance at almost all IoU levels. These results suggest two conclusions. First, $u = 0.5$ is not a good choice for precise detection, simply more robust to low quality proposals. Second, highly precise detection requires hypotheses that match the detector quality. Next, the original detector proposals were replaced by the Cascade R-CNN proposals of higher quality ($u = 0.6$ and $u = 0.7$ used the 2nd and 3rd stage proposals, respectively). Figure 5 (a) also suggests that the performance of the two detectors is significantly improved when the testing proposals closer match the detector quality.

Testing all Cascade R-CNN detectors at all cascade stages produced similar observations. Figure 6 shows that each detector was improved when used more precise hypotheses, while higher quality detector had larger gain. For example, the detector of $u = 0.7$ performed poorly for the low quality proposals of the 1st stage, but much better for the more precise hypotheses available at the deeper cascade stages. In addition, the jointly trained detectors of Figure 6 outperformed the individually trained detectors of Figure



(a)

(b)

Figure 7. (a) is the localization comparison, and (b) is the detection performance of individual classifiers in the *integral loss* detector.

	AP	AP ₅₀	AP ₆₀	AP ₇₀	AP ₈₀	AP ₉₀
FPN+ baseline	34.9	57.0	51.9	43.6	29.7	7.1
Iterative BBox	35.4	57.2	52.1	44.2	30.4	8.1
Integral Loss	35.4	57.3	52.5	44.4	29.9	6.9
Cascade R-CNN	38.9	57.8	53.4	46.9	35.8	15.8

Table 1. The comparison with *iterative BBox* and *integral loss*.

5 (a), even when the same proposals were used. This indicates that the detectors are better trained within the Cascade R-CNN framework.

5.3. Comparison with Iterative BBox and Integral Loss

In this section, we compare the Cascade R-CNN to *iterative BBox* and the *integral loss* detector. *Iterative BBox* was implemented by applying the FPN+ baseline iteratively, three times. The *integral loss* detector also has three classification heads, with $U = \{0.5, 0.6, 0.7\}$.

Localization: The localization performances of cascade regression and *iterative BBox* are compared in Figure 7 (a). The use of a single regressor degrades localization for hypotheses of high IoU. This effect accumulates when the regressor is applied iteratively, as in *iterative BBox*, and performance actually drops. Note the very poor performance of *iterative BBox* after 3 iterations. On the contrary, the cascade regressor has better performance at later stages, outperforming *iterative BBox* at almost all IoU levels.

Integral Loss: The detection performances of all classifiers in the *integral loss* detector, sharing a single regressor, are shown in Figure 7 (b). The classifier of $u = 0.6$ is the best at all IoU levels, while the classifier of $u = 0.7$ is the worst. The ensemble of all classifiers shows no visible gain.

Table 1 shows, both *iterative BBox* and *integral loss* detector improve the baseline detector marginally. The cascade R-CNN has the best performance for all evaluation metrics. The gains are mild for low IoU thresholds but significant for the higher ones.

5.4. Ablation Experiments

A couple of ablation experiments were run to analyze the proposed Cascade R-CNN.

test stage	AP	AP ₅₀	AP ₆₀	AP ₇₀	AP ₈₀	AP ₉₀
1	35.5	57.2	52.4	44.1	30.5	8.1
2	38.3	57.9	53.4	46.4	35.2	14.2
3	38.3	56.6	52.2	46.3	35.7	15.9
$\overline{1 \sim 2}$	38.5	58.2	53.8	46.7	35.0	14.0
$\overline{1 \sim 3}$	38.9	57.8	53.4	46.9	35.8	15.8
FPN+ baseline	34.9	57.0	51.9	43.6	29.7	7.1

Table 2. The stage performance of Cascade R-CNN. $\overline{1 \sim 3}$ indicates the ensemble result, which is the average of the three classifier probabilities, given the 3rd stage proposals.

IoU↑ stat	AP	AP ₅₀	AP ₆₀	AP ₇₀	AP ₈₀	AP ₉₀
	36.8	57.8	52.9	45.4	32.0	10.7
✓	38.5	58.4	54.1	47.1	35.0	13.1
✓	37.5	57.8	53.1	45.5	33.3	13.1
✓ ✓	38.9	57.8	53.4	46.9	35.8	15.8

Table 3. The ablation experiments. “IoU↑” means increasing IoU thresholds, and “stat” exploiting sequential regression statistics.

Stage-wise Comparison: Table 2 summarizes stage performance. Note that the 1st stage already outperforms the baseline detector, due to the benefits of multi-stage multi-task learning. Deeper cascade stages prefer higher quality localization, encouraging to learn features conducive to it. This benefits earlier cascade stages by features sharing across stages. The 2nd stage improves performance substantially, and the 3rd is equivalent to the 2nd. This differs from the *integral loss* detector, where the higher IoU classifier is relatively weak. While the former (later) stage is better at low (high) IoU metrics, the ensemble of all classifiers is the best overall.

IoU Thresholds: A preliminary Cascade R-CNN was trained using the same IoU threshold $u = 0.5$ for all heads. In this case, the stages differ only in the hypotheses they receive. Each stage is trained with the corresponding hypotheses, i.e. accounting for the distributions of Figure 2. The first row of Table 3 shows that the cascade improves on the baseline detector. This suggests the importance of optimizing stages for the corresponding sample distributions. The second row shows that, by increasing the stage threshold u , the detector can be made more selective against close false positives and *specialized* for more precise hypotheses, leading to additional gains. This supports the conclusions of Section 4.2.

Regression Statistics: Exploiting the progressively updated regression statistics, of Figure 2, helps the effective multi-task learning of classification and regression. Its benefit is noted by comparing the models with/without it in Table 3. The learning is not sensitive to these statistics.

Number of Stages: The impact of the number of stages is summarized in Table 4. Adding a second detection stage significantly improves the baseline detector. Three detection stages still produce non-trivial improvement, but the

# stages	test stage	AP	AP ₅₀	AP ₆₀	AP ₇₀	AP ₈₀	AP ₉₀
1	1	34.9	57.0	51.9	43.6	29.7	7.1
2	$\overline{1 \sim 2}$	38.2	58.0	53.6	46.7	34.6	13.6
3	$\overline{1 \sim 3}$	38.9	57.8	53.4	46.9	35.8	15.8
4	$\overline{1 \sim 3}$	38.9	57.4	53.2	46.8	36.0	16.0
4	$\overline{1 \sim 4}$	38.6	57.2	52.8	46.2	35.5	16.3

Table 4. The impact of the number of stages in Cascade R-CNN.

addition of a 4th stage ($u = 0.75$) led to a slight performance decrease. Note, however, that while the overall AP performance degrades, the four-stage cascade has the best performance for high IoU levels. The three-stage cascade achieves the best trade-off.

5.5. Comparison with the state-of-the-art

The Cascade R-CNN, based on FPN+ and ResNet-101 backbone, is compared to state-of-the-art *single-model* object detectors in Table 5. The settings are as described in Section 5.1.1, but a total of 280k training iterations were run and the learning rate dropped at 160k and 240k iterations. The number of RoIs was also increased to 512. The first group of detectors on Table 5 are one-stage detectors, the second group two-stage, and the last group multi-stage (3-stages+RPN for the Cascade R-CNN). All the compared state-of-the-art detectors were trained with $u = 0.5$. It is noted that our FPN+ implementation is better than the original FPN [23], providing a very strong baseline. In addition, the extension from FPN+ to Cascade R-CNN improved performance by ~ 4 points. The Cascade R-CNN also outperformed all *single-model* detectors by a large margin, under all evaluation metrics. This includes the *single-model* entries of the COCO challenge winners (Faster R-CNN++ [18], and G-RMI [19]), and the very recent Deformable R-FCN [5], RetinaNet [24] and Mask R-CNN [16]. Compared to the best multi-stage detector on COCO, AttractioNet [11], although it used many enhancements, the vanilla Cascade R-CNN still outperforms it by 7.1 points. Note that, unlike Mask R-CNN, no segmentation information is exploited in the Cascade R-CNN. Finally, the vanilla *single-model* Cascade R-CNN also surpasses the heavily engineered ensemble detectors that won the COCO challenge in 2015 and 2016 (AP 37.4 and 41.6, respectively)¹.

5.6. Generalization Capacity

Three-stage Cascade R-CNN of all three baseline detectors are compared in Table 6. All settings are as above, with the changes of Section 5.5 for FPN+.

Detection Performance: Again, our implementations are better than the original detectors [30, 4, 23]. Still, the Cascade R-CNN improves on these baselines consistently by 2~4 points, independently of their strength. These gains

¹<http://cocodataset.org/#detections-leaderboard>

	backbone	AP	AP ₅₀	AP ₇₅	AP _S	AP _M	AP _L
YOLOv2 [29]	DarkNet-19	21.6	44.0	19.2	5.0	22.4	35.5
SSD513 [25]	ResNet-101	31.2	50.4	33.3	10.2	34.5	49.8
RetinaNet [24]	ResNet-101	39.1	59.1	42.3	21.8	42.7	50.2
Faster R-CNN+++ [18]*	ResNet-101	34.9	55.7	37.4	15.6	38.7	50.9
Faster R-CNN w FPN [23]	ResNet-101	36.2	59.1	39.0	18.2	39.0	48.2
Faster R-CNN w FPN+ (ours)	ResNet-101	38.8	61.1	41.9	21.3	41.8	49.8
Faster R-CNN by G-RMI [19]	Inception-ResNet-v2	34.7	55.5	36.7	13.5	38.1	52.0
Deformable R-FCN [5]*	Aligned-Inception-ResNet	37.5	58.0	40.8	19.4	40.1	52.5
Mask R-CNN [16]	ResNet-101	38.2	60.3	41.7	20.1	41.1	50.2
AttractioNet [11]*	VGG16+Wide ResNet	35.7	53.4	39.3	15.6	38.0	52.7
Cascade R-CNN	ResNet-101	42.8	62.1	46.3	23.7	45.5	55.2

Table 5. The state-of-the-art *single-model* detectors on COCO `test-dev`. The entries denoted by “*” used bells and whistles at inference.

	backbone	cascade	train speed	test speed	model size	val (5k)						test-dev (20k)					
						AP	AP ₅₀	AP ₇₅	AP _S	AP _M	AP _L	AP	AP ₅₀	AP ₇₅	AP _S	AP _M	AP _L
Faster R-CNN	VGG	✗	0.12s	0.075s	278M	23.6	43.9	23.0	8.0	26.2	35.5	23.5	43.9	22.6	8.1	25.1	34.7
		✓	0.14s	0.115s	704M	27.0	44.2	27.7	8.6	29.1	42.2	26.9	44.3	27.8	8.3	28.2	41.1
R-FCN	ResNet-50	✗	0.19s	0.07s	133M	27.0	48.7	26.9	9.8	30.9	40.3	27.1	49.0	26.9	10.4	29.7	39.2
		✓	0.24s	0.075s	184M	31.1	49.8	32.8	10.4	34.4	48.5	30.9	49.9	32.6	10.5	33.1	46.9
R-FCN	ResNet-101	✗	0.23s	0.075s	206M	30.3	52.2	30.8	12.0	34.7	44.3	30.5	52.9	31.2	12.0	33.9	43.8
		✓	0.29s	0.083s	256M	33.3	52.0	35.2	11.8	37.2	51.1	33.3	52.6	35.2	12.1	36.2	49.3
FPN+	ResNet-50	✗	0.30s	0.095s	165M	36.5	58.6	39.2	20.8	40.0	47.8	36.5	59.0	39.2	20.3	38.8	46.4
		✓	0.33s	0.115s	272M	40.3	59.4	43.7	22.9	43.7	54.1	40.6	59.9	44.0	22.6	42.7	52.1
FPN+	ResNet-101	✗	0.38s	0.115s	238M	38.5	60.6	41.7	22.1	41.9	51.1	38.8	61.1	41.9	21.3	41.8	49.8
		✓	0.41s	0.14s	345M	42.7	61.6	46.6	23.8	46.2	57.4	42.8	62.1	46.3	23.7	45.5	55.2

Table 6. Detailed comparison on multiple popular baseline object detectors. All speeds are reported per image on a single Titan Xp GPU.

backbone	Faster R-CNN		R-FCN				
	AlexNet	VGG	RetNet-50	RetNet-101			
cascade	✗	✓	✗	✓	✗	✓	
AP	29.4	38.9	42.9	51.2	44.8	51.8	49.4
AP ₅₀	63.2	66.5	76.4	79.1	77.5	78.5	79.8
AP ₇₅	23.7	40.5	44.1	56.3	46.8	57.1	53.2
							59.2

Table 7. Detection results on PASCAL VOC 2007 `test`.

are also consistent on `val` and `test-dev`. These results suggest that the Cascade R-CNN is widely applicable across detector architectures.

Parameter and Timing: The number of the Cascade R-CNN parameters increases with the number of cascade stages. The increase is linear in the parameter number of the baseline detector heads. In addition, because the computational cost of a detection head is usually small when compared to the RPN, the computational overhead of the Cascade R-CNN is small, at both training and testing.

5.7. Results on PASCAL VOC

The Cascade R-CNN was further experimented on PASCAL VOC dataset [8]. Following [30, 25], the models were trained on VOC2007 and VOC2012 `trainval` and tested on VOC2007 `test`. Faster R-CNN (with AlexNet and VGG-Net) and R-FCN (with ResNet) were tested. The training details were similar to Section 5.1.1, and AlexNet were also pruned. Since the goal of this paper is to explore

high quality detection, we used the COCO metrics for evaluation². The detection results in Table 7 show that the Cascade R-CNN also has significant improvements over multiple detection architectures on PASCAL VOC. These reinforce our belief on the robustness of the Cascade R-CNN.

6. Conclusion

In this paper, we proposed a multi-stage object detection framework, the Cascade R-CNN, for the design of high quality object detectors. This architecture was shown to avoid the problems of overfitting at training and quality mismatch at inference. The solid and consistent detection improvements of the Cascade R-CNN on the challenging COCO and the popular PASCAL VOC datasets suggest the modeling and understanding of various concurring factors are required to advance object detection. The Cascade R-CNN was shown to be applicable to many object detection architectures. We believe that it can be useful to many future object detection research efforts.

Acknowledgment This work was funded by NSF Awards IIS-1208522 and IIS-1637941, ONR award UCSD-SUBK-N141-076, and a GPU donation from NVIDIA. We also would like to thank Kaiming He for valuable discussions.

²The annotations of PASCAL VOC were transformed to COCO format, and COCO toolbox was used for evaluation. The results are different from the original VOC evaluation.

References

- [1] Z. Cai, Q. Fan, R. S. Feris, and N. Vasconcelos. A unified multi-scale deep convolutional neural network for fast object detection. In *ECCV*, pages 354–370, 2016. 2, 3
- [2] X. Cao, Y. Wei, F. Wen, and J. Sun. Face alignment by explicit shape regression. In *CVPR*, pages 2887–2894, 2012. 4
- [3] J. Dai, K. He, and J. Sun. Instance-aware semantic segmentation via multi-task network cascades. In *CVPR*, pages 3150–3158, 2016. 3
- [4] J. Dai, Y. Li, K. He, and J. Sun. R-FCN: object detection via region-based fully convolutional networks. In *NIPS*, pages 379–387, 2016. 2, 3, 5, 7
- [5] J. Dai, H. Qi, Y. Xiong, Y. Li, G. Zhang, H. Hu, and Y. Wei. Deformable convolutional networks. In *ICCV*, 2017. 7, 8
- [6] P. Dollár, P. Welinder, and P. Perona. Cascaded pose regression. In *CVPR*, pages 1078–1085, 2010. 4
- [7] C. Elkan. The foundations of cost-sensitive learning. In *IJCAI*, pages 973–978, 2001. 2
- [8] M. Everingham, L. J. V. Gool, C. K. I. Williams, J. M. Winn, and A. Zisserman. The pascal visual object classes (VOC) challenge. *International Journal of Computer Vision*, 88(2):303–338, 2010. 8
- [9] P. F. Felzenszwalb, R. B. Girshick, D. A. McAllester, and D. Ramanan. Object detection with discriminatively trained part-based models. *IEEE Trans. Pattern Anal. Mach. Intell.*, 32(9):1627–1645, 2010. 2
- [10] S. Gidaris and N. Komodakis. Object detection via a multi-region and semantic segmentation-aware CNN model. In *ICCV*, pages 1134–1142, 2015. 3
- [11] S. Gidaris and N. Komodakis. Attend refine repeat: Active box proposal generation via in-out localization. In *BMVC*, 2016. 3, 7, 8
- [12] S. Gidaris and N. Komodakis. Locnet: Improving localization accuracy for object detection. In *CVPR*, pages 789–798, 2016. 3
- [13] R. B. Girshick. Fast R-CNN. In *ICCV*, pages 1440–1448, 2015. 1, 2, 3, 5
- [14] R. B. Girshick, J. Donahue, T. Darrell, and J. Malik. Rich feature hierarchies for accurate object detection and semantic segmentation. In *CVPR*, pages 580–587, 2014. 1, 2
- [15] S. Han, J. Pool, J. Tran, and W. J. Dally. Learning both weights and connections for efficient neural network. In *NIPS*, pages 1135–1143, 2015. 5
- [16] K. He, G. Gkioxari, P. Dollár, and R. Girshick. Mask r-cnn. In *ICCV*, 2017. 3, 5, 7, 8
- [17] K. He, X. Zhang, S. Ren, and J. Sun. Spatial pyramid pooling in deep convolutional networks for visual recognition. In *ECCV*, pages 346–361, 2014. 2
- [18] K. He, X. Zhang, S. Ren, and J. Sun. Deep residual learning for image recognition. In *CVPR*, pages 770–778, 2016. 3, 5, 7, 8
- [19] J. Huang, V. Rathod, C. Sun, M. Zhu, A. Korattikara, A. Fathi, I. Fischer, Z. Wojna, Y. Song, S. Guadarrama, and K. Murphy. Speed/accuracy trade-offs for modern convolutional object detectors. *CoRR*, abs/1611.10012, 2016. 7, 8
- [20] Y. Jia, E. Shelhamer, J. Donahue, S. Karayev, J. Long, R. B. Girshick, S. Guadarrama, and T. Darrell. Caffe: Convolutional architecture for fast feature embedding. In *MM*, pages 675–678, 2014. 5
- [21] H. Li, Z. Lin, X. Shen, J. Brandt, and G. Hua. A convolutional neural network cascade for face detection. In *CVPR*, pages 5325–5334, 2015. 3
- [22] T. Lin, M. Maire, S. J. Belongie, J. Hays, P. Perona, D. Ramanan, P. Dollár, and C. L. Zitnick. Microsoft COCO: common objects in context. In *ECCV*, pages 740–755, 2014. 2, 5
- [23] T.-Y. Lin, P. Dollár, R. Girshick, K. He, B. Hariharan, and S. Belongie. Feature pyramid networks for object detection. In *CVPR*, 2017. 1, 2, 3, 5, 7, 8
- [24] T.-Y. Lin, P. Goyal, R. Girshick, K. He, and P. Dollár. Focal loss for dense object detection. In *ICCV*, 2017. 3, 7, 8
- [25] W. Liu, D. Anguelov, D. Erhan, C. Szegedy, S. E. Reed, C. Fu, and A. C. Berg. SSD: single shot multibox detector. In *ECCV*, pages 21–37, 2016. 2, 8
- [26] H. Masnadi-Shirazi and N. Vasconcelos. Cost-sensitive boosting. *IEEE Trans. Pattern Anal. Mach. Intell.*, 33(2):294–309, 2011. 2
- [27] M. Najibi, M. Rastegari, and L. S. Davis. G-CNN: an iterative grid based object detector. In *CVPR*, pages 2369–2377, 2016. 3
- [28] W. Ouyang, K. Wang, X. Zhu, and X. Wang. Learning chained deep features and classifiers for cascade in object detection. *CoRR*, abs/1702.07054, 2017. 3
- [29] J. Redmon, S. K. Divvala, R. B. Girshick, and A. Farhadi. You only look once: Unified, real-time object detection. In *CVPR*, pages 779–788, 2016. 2, 8
- [30] S. Ren, K. He, R. B. Girshick, and J. Sun. Faster R-CNN: towards real-time object detection with region proposal networks. In *NIPS*, pages 91–99, 2015. 1, 2, 3, 4, 5, 7, 8
- [31] A. Shrivastava, A. Gupta, and R. B. Girshick. Training region-based object detectors with online hard example mining. In *CVPR*, pages 761–769, 2016. 5
- [32] K. Simonyan and A. Zisserman. Very deep convolutional networks for large-scale image recognition. *CoRR*, abs/1409.1556, 2014. 5
- [33] J. R. R. Uijlings, K. E. A. van de Sande, T. Gevers, and A. W. M. Smeulders. Selective search for object recognition. *International Journal of Computer Vision*, 104(2):154–171, 2013. 4
- [34] P. A. Viola and M. J. Jones. Robust real-time face detection. *International Journal of Computer Vision*, 57(2):137–154, 2004. 2, 3
- [35] J. Yan, Z. Lei, D. Yi, and S. Li. Learn to combine multiple hypotheses for accurate face alignment. In *ICCV Workshops*, pages 392–396, 2013. 4
- [36] B. Yang, J. Yan, Z. Lei, and S. Z. Li. CRAFT objects from images. In *CVPR*, pages 6043–6051, 2016. 3
- [37] D. Yoo, S. Park, J. Lee, A. S. Paek, and I. Kweon. Attention-net: Aggregating weak directions for accurate object detection. In *ICCV*, pages 2659–2667, 2015. 3
- [38] S. Zagoruyko, A. Lerer, T. Lin, P. O. Pinheiro, S. Gross, S. Chintala, and P. Dollár. A multipath network for object detection. In *BMVC*, 2016. 4